FARADAY

Effect of temperature on crystal growth and crystal properties of paracetamol

Boris Yu. Shekunov,[a,*] Michael E. Aulton,[a] Robert W. Adama-Acquah[a] and David J. W. Grant[b]

[a] *Department of Pharmaceutical Sciences, Department of Physics, De Montfort University, Leicester, UK LE1 9BH*

[b] *Department of Pharmaceutics, College of Pharmacy, University of Minnesota, Health Sciences Unit F, 308 Harvard Street S.E., Minneapolis, MN 55455-0343, USA*

The crystal growth kinetics of paracetamol have been investigated at different temperatures and the crystals obtained have been analysed for their mechanical properties. Variations in the crystal habit and crystal quality can be explained by different growth activation energies for the most important crystallographic faces, {001} and {110}. The magnitude of these energies corresponds to the anisotropy of the intermolecular bonds in the crystal lattice. The crystallization temperature strongly influences the thermodynamic and mechanical properties of paracetamol crystals.

In crystallization from solution, supersaturation is usually generated by controlling the solution temperature. This results in a combined influence of both temperature and supersaturation on growth processes. The examination of supersaturation dependences at different temperatures enables these two phenomena to be distinguished. Since all kinetic parameters exhibit temperature dependences, such a study will provide valuable information about the growth activation energy as well as the character of any impurity and solvent adsorption. This method has been employed for the investigation of potassium and ammonium phosphates[1–3] and L-arginine chloride.[4] An *in situ* interferometric technique enables the growth step velocity to be measured as a function of temperature and the step kinetic coefficient to be determined from the linearity of this function. For molecular organic crystals the behaviour of growth velocity is non-linear and complex.[5–7]

The present work consists of two parts. First, the effect of temperature on the growth kinetics of paracetamol crystal faces is investigated. In the second part, certain mechanical crystal properties are studied with respect to the crystallization conditions. Paracetamol (monoclinic, space group $P2_1/a$) is a widely used non-steroidal analgesic drug which is a typical representative of organic drug substances composed of aromatic polyfunctional molecules. Such drugs are usually administrated as tablets. As a result, physicochemical variations produced by changing the crystallization temperature will have a direct impact on industrial formulation problems, such as bioinequivalence (influenced by variable dissolution rate), porosity and tablet compression problems.

Experimental

Crystal growth measurements

Surface kinetic measurements were carried out using a specially designed optical cell shown in Fig. 1(a). The principle of the measurements is similar to that of the Michelson interferometer whereby the crystal face under investigation is used as the reflecting surface in one arm of the interferometer. This arrangement results in the production of a 'topographic map' of the crystal surface as shown in Fig. 1(b) and (c). The distance between interferometric fringes gives the steepness of the growth hillocks, p, whereas the movement of the fringes in the normal and tangential directions as a function of time allows the growth rate, R, and the growth step velocity, v, respectively, to be measured. The crystal habit of paracetamol was determined using optical goniometry as shown in Fig. 2. The major crystallization parameters R, p and v were obtained as functions of both supersaturation and temperature for the most important crystal faces of paracetamol, *i.e.* {001} and {110}.

The experimental procedure is illustrated in Fig. 3. For each crystal face, measurements began at the highest equilibrium temperature. The temperature was then decreased to the point of maximum possible growth velocity without nucleation. The solution was then diluted step by step at a constant temperature shown by one of the horizontal lines in Fig. 3 until a

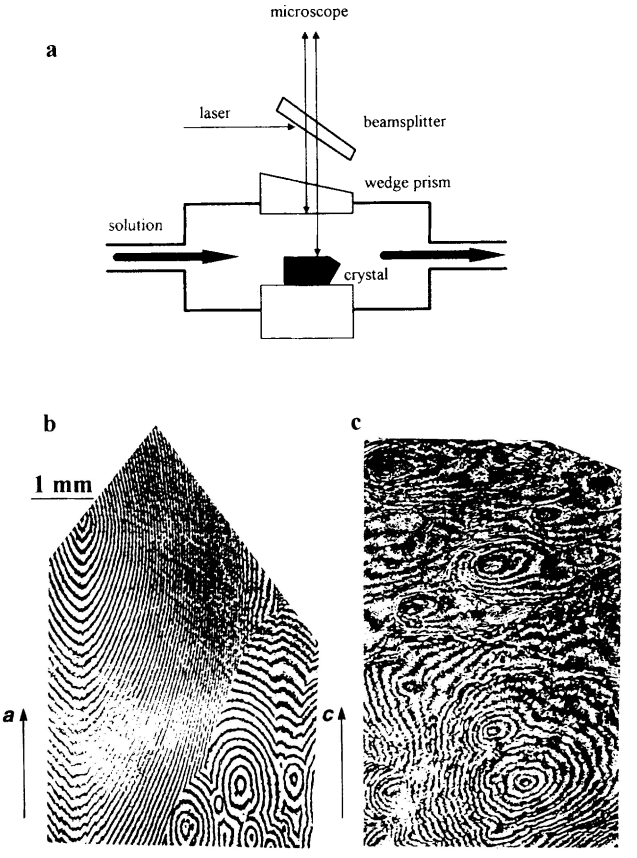

Fig. 1 (a) Optical cell used for the interferometric measurements; (b), and (c), typical interferograms of the (001) and (110) crystal surfaces, respectively, at *ca.* 47 °C

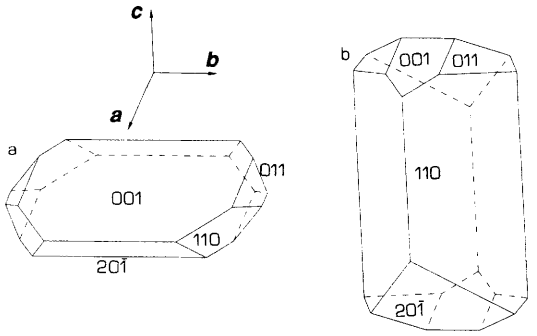

Fig. 2 Miller indices of paracetamol crystals grown at 3 °C (a) and at 47 °C (b)

new equilibrium was reached. The supersaturation σ was calculated by the equation:

$$\sigma = \ln(c/c_0) \quad (1)$$

where c and c_0 are the actual and saturated concentrations, respectively, of the solution in mol.% reported elsewhere.[8]

The optical scheme employed has a number of advantages over the Michelson interferometer used previously.[1,3–7] A considerable problem for precise measurement of interferometric fringes arises when vibrations are produced by pumping a solution through the crystallization cell. This problem is solved in the new cell. The optical window [wedge prism in Fig. 1(a)] is also a reference mirror for the interferometer. Since the reflecting crystal surface and the mirror are combined in a single unit, all internal and external vibrations are completely eliminated. This scheme is also simpler than the Michelson interferometer, does not require special optical accessories, and allows better control over temperature during crystallization.

Paracetamol (4-acetamidophenol), 98%, was obtained from Aldrich and then purified by recrystallizing several times in ethanol. Some differences from the previous measurements with paracetamol supplied by Sigma Chemicals[6,7] were noticed. Both materials, although purified, may contain minute quantities of impurities. These impurities, however, did not change the fundamental characteristics of the growth dependences such as the magnitude of the kinetic coefficient and growth anisotropy.

Preparation of crystals

Crystals for thermoanalysis and mechanical measurements were grown by slow evaporation in a thermostatically controlled flask at two temperatures, 47 and 3 °C (±0.1 °C). The crystallization conditions were selected to provide a constant growth rate of *ca.* 5×10^{-8} m s^{-1} at both temperatures. These conditions corresponded to the average supersaturation

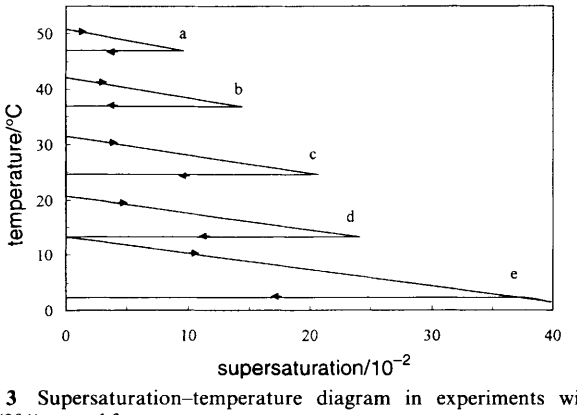

Fig. 3 Supersaturation–temperature diagram in experiments with the (001) crystal face

during the measurement of the growth kinetics. The growth rate was continuously monitored under a microscope. When the size of the crystals had reached 3–4 mm, the crystals were removed and used for further examinations. The {001} crystal shape dominated at 3 °C, whereas the {110} shape dominated at 47 °C.

Differential scanning calorimetry (DSC) and thermogravimetry

Measurements of the enthalpy of fusion, $\Delta_f H$, and melting point, T_m, of milled paracetamol crystals (8–10 mg) were carried out in sealed aluminium pans heated at a rate of 5 °C min^{-1} (41.84 mJ s^{-1}) in a Perkin-Elmer DSC-4 calorimeter using indium (6 mg) as the calorimetric standard. From the single observed endotherm, T_m of the crystals was taken to be the temperature at the point of intersection of the leading line of steepest slope and the base line. $\Delta_f H$ of the crystals was calculated from the peak area which was determined by cutting and weighing. The precision of this procedure was *ca.* 0.5%.

The content of water in the paracetamol crystals was measured using thermobalances and heating paracetamol above the melting point. Paracetamol did not undergo structural decomposition up to and beyond the melting point: (*a*) the DSC endotherms and baselines remained the same for the solidified melt and for the pure paracetamol crystals, (*b*) paracetamol material retained its weight after several successful solidifications. Thus, the lost weight of paracetamol crystals corresponded to the water content.

Indentation and crushing techniques

The mechanical properties of paracetamol crystals were examined first using a microindentation apparatus.[9] It consisted of a spherical sapphire indentor (diameter $D = 1.55$ mm) which was loaded onto the test surface under a selected load (optimum $F = 1$ N). The depth of the indentation (h_1) and the recovery (δh) when the load was removed were both measured directly by a transducer.[10] In parallel, the final depth of indentation was also calculated by measuring the diameter of indentation under the microscope. Both methods gave identical results for h_1 and, thus, indicated that deformation of the indentor itself was negligible. The measurements were quantified in terms of Brinell hardness (HB), modulus of elasticity (E_{elast}) and elastic quotient (Q_{elast}) according to:[9]

$$\mathrm{HB} = F/(\pi D h_1) \quad (2)$$

$$E_{elast} = 0.3419F/[\delta h\sqrt{(D)h_1}] \quad (3)$$

$$Q_{elast} = \delta h/h_1 \quad (4)$$

The test was conducted on the crystal faces {001} and {110}, the face under investigation being oriented perpendicular to the direction of indentation. At least four indentations were made for each crystal face and *ca.* 20 different crystals were tested and the mean value obtained. It should be noted that values of HB and E_{elast} showed deviations of *ca.* 50% for both crystal shapes. This high deviation has been recorded previously in similar experiments.[9] Although cracking of the crystal was avoided as far as possible, crystal inhomogeneities such as solution inclusions significantly influenced the results.

The second mechanical test was carried out using the single-particle crushing assembly. This consisted of a highly sensitive load cell (U-4000, Maywood Instruments Ltd.) which was sensitive to a maximum load of 50 N and capable of a high dynamic response within this interval. A motorised unit, to which an upper steel piston was connected, was set to approach the crystal mounted on a lower platen at a given strain rate. The force was applied onto the face under investigation. The crystal displacement and load applied were moni-

tored on the x and y axes, respectively, of a chart recorder. The recorder was calibrated at the beginning of the experiment and the results were corrected for machine deformation. The proportionality coefficient between the elastic strain, ε, exhibited by a crystal on the application of a loading stress, s, enabled the elasticity modulus to be determined. The magnitudes of ε and s were calculated from the applied force and crystal dimensions. In addition, the critical stress s_C needed to produce fracture of the crystal was determined and the work done, W, in causing the crystal fracture was calculated from the area under the curve. These measurements were conducted on *ca.* 20 different crystals.

Results

Growth kinetics

The velocity of growth steps, v, is the most important quantity describing the growth kinetics and temperature dependence. The other independent growth parameter, surface steepness p, was found to be a function of dislocation activity and varied from crystal to crystal. Since p showed a much weaker dependence on temperature than v, the growth rate, $R = pv$, and crystal shape were mostly defined by the $v(\sigma, T)$ functions.

Fig. 4(a) shows the dependences $v(\sigma, T)$ for the (001) face. Supersaturation was introduced by varying the concentration. The dependences were found to be linear functions of supersaturation. Crystal growth, however, did not start at zero σ. This behaviour is different from the proportionality between v and σ observed for inorganic materials.[1–3]

Fig. 4(b) gives the growth velocity dependences *vs.* temperature on the (110) face. These dependences are clearly non-linear with a broad zone of zero velocities and a very rapid velocity increase after supersaturation exceeds some critical value, σ_C.

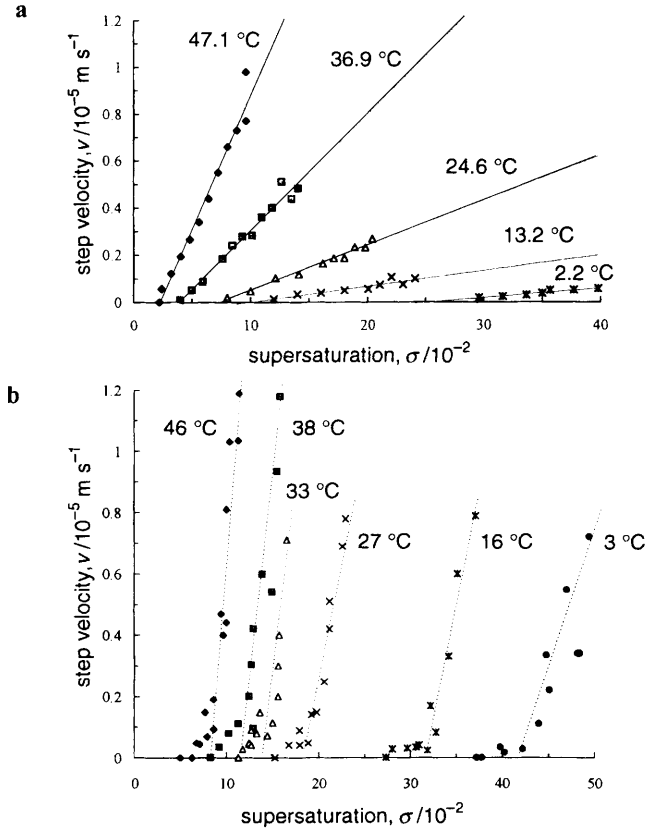

Fig. 4 Velocity of growth steps v[010] on the (001) (a) and (110) (b) crystal faces as a function of supersaturation σ at different temperature. The lines show the slopes of these functions.

Dependences similar to those in Fig. 4 were also obtained when supersaturation was varied by a decrease of temperature (corresponding to the horizontal lines in Fig. 3). The kinetics showed no significant difference with those observed for the concentration variation, probably because of the relatively narrow temperature interval.

According to crystal growth theory,[11] the dependence of the step velocity–supersaturation slope (Fig. 4) on temperature can be expressed in Arrhenius coordinates:

$$\delta \ln(\delta v/\delta\sigma)/\delta(1/T) = -(E + \Delta_d H)/R_g \qquad (5)$$

where E is the activation energy of the growth kinetic coefficient, $\Delta_d H = 22.47$ kJ mol^{-1} is the enthalpy of dissolution obtained from the solubility data[8] and R_g is the gas constant. Arrhenius plots are shown in Fig. 5A. The slope of curve 1 gives the activation energy value $E(001)_b = 33.6$ kJ mol^{-1} for the growth velocity in the [010] crystallographic direction on the (001) face (squared correlation coefficient 0.98). Similar data obtained for the [100] growth steps on the (001) face (curve 2) give $E(001)_a = 46.0$ kJ mol^{-1}.

Determination of activation energy for the (110) face is less reliable owing to a distinct non-linearity of $v(\sigma)$. The mean activation energy can be calculated from the slopes at high supersaturation [broken lines in Fig. 4(b)]. The Arrhenius plot in Fig. 5A (curve 3) gives a very small value of activation energy $E(110) = 0.3$ kJ mol^{-1} for the (110) face in the direction [001].

The second important characteristic of the growth dependences in Fig. 4(a) and (b) is the critical supersaturation σ_C below which the crystals cannot grow. A function, similar to that of Arrhenius dependence, can be obtained for this quantity. According to the definition of supersaturation (1), σ_C can

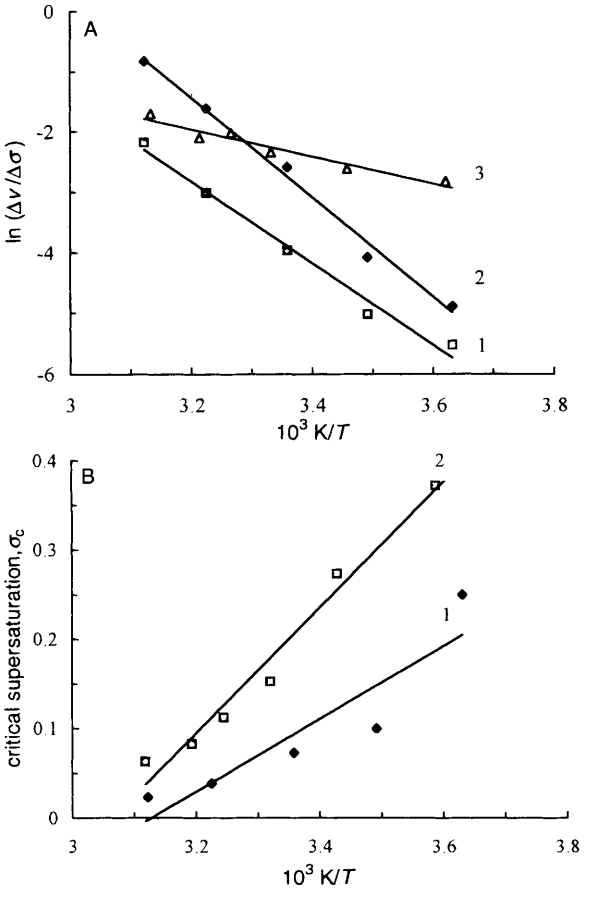

Fig. 5 A, Slope of growth velocity $\Delta v/\Delta\sigma$ *vs.* $1/T$ for the (001) crystal face in two perpendicular directions (curves 1 and 2) and for the (110) crystal face (curve 3). B, Critical supersaturation of growth σ_C *vs.* $1/T$ for the (001) face (curve 1) and (110) face (curve 2).

be directly related to the change in the Gibbs energy ΔG which is needed to initiate crystal growth:

$$\Delta G/R_g T = \sigma_C \quad (6)$$

Application of the Gibbs–Helmholtz equation leads to:

$$\Delta\sigma_C/\Delta(1/T) = -U/R_g \quad (7)$$

The energy, U, describes the variation of σ_C with temperature and plays a role similar to that of the activation energy. From Fig. 5B the values $U(001) = 3.4$ kJ mol^{-1} and $U(100) = 5.8$ kJ mol^{-1} are obtained.

The different character of the growth dependences for the (001) and (110) faces has a great impact on the crystal habit and crystal quality of paracetamol. At *ca.* 3 °C the crystals showed a plate-llke habit with dominant {001} faces [Fig. 6(a)]. At *ca.* 47 °C the crystals had a distinct prismatic shape with developed {110} faces [Fig. 6(b)]. The crystals grown at a lower temperature exhibited a high degree of translucency as compared to the relatively transparent crystals obtained at a higher temperature. These changes can be associated with the very different activation energies for the investigated faces. Fig. 7 shows the growth rate of the (001) and (110) faces at the two temperatures. At 47 °C, the {110} faces grew, on average, slower than the {001} faces because of their larger σ_C value. As the temperature decreased and the supersaturation increased, the growth velocity on the {001} faces became smaller than that on the {110} faces. The very large values of σ_C at a lower temperature may indicate a stronger interaction between the crystal faces and water and results in incorporation of solvent inclusions into the crystals.

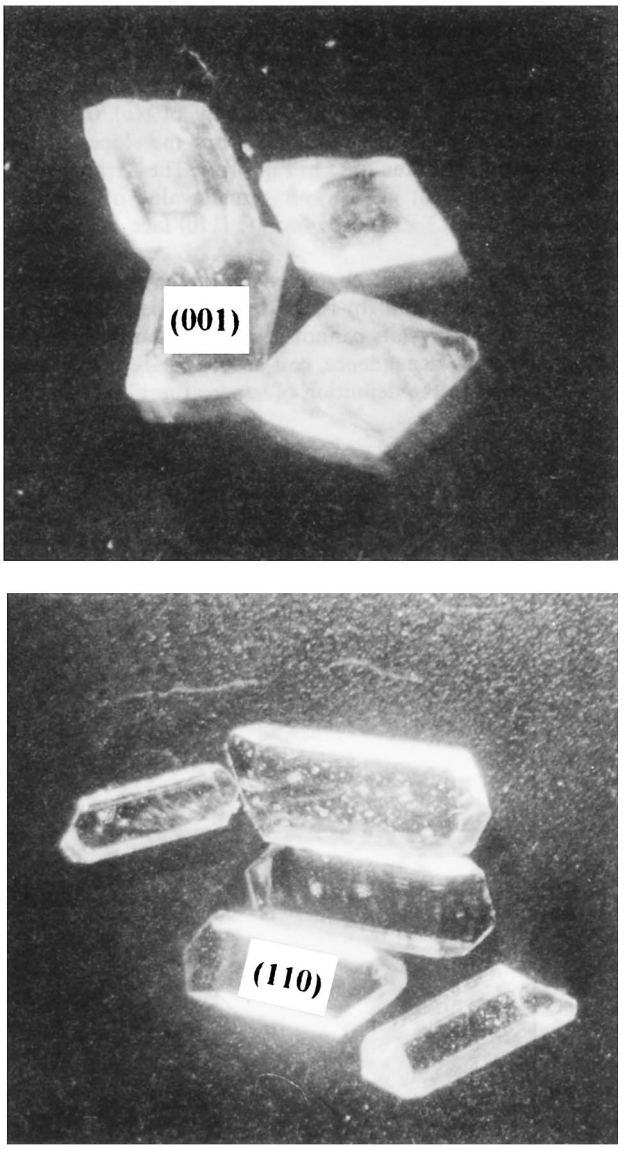

Fig. 6 Habit of paracetamol crystals obtained at 3 °C (a) (upper) and at 47 °C (b) (lower)

Enthalpy of fusion and mechanical properties

The data obtained for the thermodynamic and mechanical properties of paracetamol crystals are summarised in Table 1. The growth defects strongly influence the observed properties. Thus, the smaller values of $\Delta_f H$ and T_m for the plate-like shapes can be associated with the formation of solution inclusions at 3 °C. These inclusions could be observed readily under the microscope and could explain the wider endotherm for the plate-like crystals than that observed for the prismatic crystals. This is also in agreement with the water content measured by thermogravimetry. An almost ten-fold increase of water content was observed for the plate-like crystals.

The prismatic crystals showed favourable mechanical properties, since they are harder and more elastic than the plate-like crystals (compare HB, E_{elast} and Q_{elast}). The values of HB and E_{elast} are notably smaller (*ca.* 10 times) than the Vickers hardness number and elasticity modulus previously reported.[12] These differences are related to the geometry and penetration characteristics of the spherical (Brinell) and pyramidal (Vickers) indentors. Paracetamol is a very brittle material; it unavoidably forms microscopic cracks around the indentation area. These cracks may contribute to the penetra-

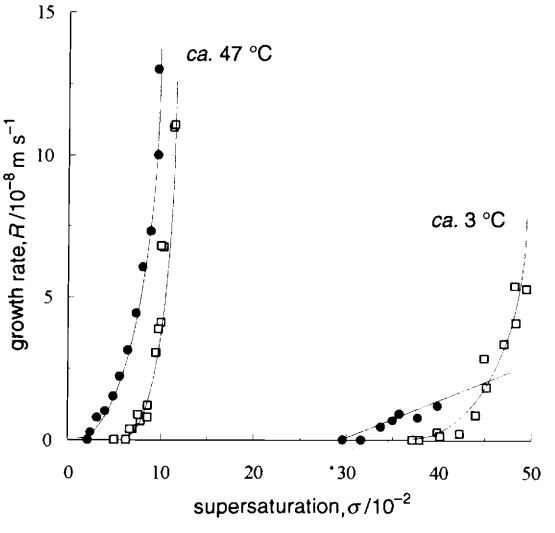

Fig. 7 Dependence of normal growth rate R on supersaturation σ for the (001) (●) and (110) (□) crystal faces at different temperatures

Table 1 Some mechanical and thermodynamic properties of paracetamol single crystals grown at two different temperatures

temperature and shape	water content (wt.%)	$\Delta_f H$/kJ mol^{-1}	T_m/°C	HB/MPa	Q_{elast}	$E_{elast}{}^a$/GPa	$E_{elast}{}^b$/GPa	s_C/MPa	W/mJ
3 °C, {001}	0.4	25.47	168.4	14.8	0.49	0.42	0.21	1.0	2.4
47 °C, {110}	5	26.14	169.5	34.7	0.65	0.72	0.29	3.2	18.1

[a] Obtained from Brinell test; [b] obtained from crushing test.

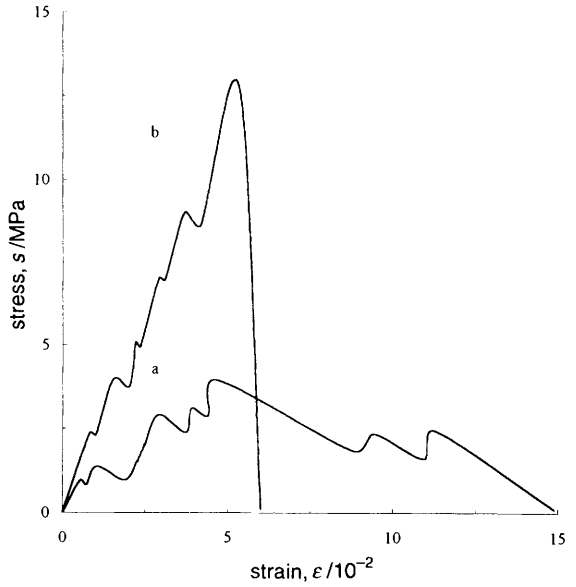

Fig. 8 Typical stress–strain plot obtained during crushing assembly test for the {001} (curve 1) and {110} (curve 2) crystal forms

tion depth of an indentor. The latter may be a source of inconsistencies between the absolute value of the mechanical parameters, particularly the elastic modulus. There is no doubt, however, that the relative parameters show much higher elasticity and hardness for the prismatic form.

The crushing test gives data that are most representative in a practical sense. This is because the test directly related to the compression and tabletting behaviour of the material. The crushing behaviour of the crystals grown at high and low temperatures is significantly different. Fig. 8 shows typical stress–strain dependences. The plate-like crystals (curve a) started to be crushed at a relatively low stress and gradually developed a large number of fractures until they completely disintegrated. The prismatic crystals (curve b) underwent relatively few fractures and suddenly collapsed at a high stress. The stress needed to develop the first crack, s_C, and the work done, W, are much greater for this prismatic crystal that for the platelet (see Table 1). The elastic modulus obtained from the linear initial portions of these curves is somewhat smaller but close to that obtained in the Brinell test. The more perfect prismatic crystals always fractured along the {010} cleavage planes, whereas the plate-like crystals showed both cleavage crushing and crushing on the inhomogeneous defects. The greater the number of such defects, the smaller stress needed to fracture the crystals. Data in Table 1 show that important processing characteristics, such as s_C and W, differ by an appreciable factor for the crystals obtained at high and low temperature.

Discussion

Relationship between the crystal structure and activation energies

The results show that the key factor defining the growth rate, crystal habit and crystal quality is the magnitude of the activation energies, E and U. The overall activation growth energy, E, depends on a number of thermodynamic and kinetic factors which can be subdivided into two groups. The first group consists of the properties independent of crystallographic orientation, such as the enthalpy of dissolution, $\Delta_d H$, and the activation energy of solvent complexes, E_S. The other factors are crystallographically specific, for example the energy of adsorption, ϕ, and the energy of formation of step kinks, w. In general, these energies appear in exponential functions of the type $\exp(-E_i/RT)$ and, therefore, will contribute to the overall activation energy of the growth velocity. Qualitatively, the expressions for the kinetic coefficient β[11]

$$\ln \beta \sim -(w + E_s + \Delta_d H - \phi)/RT \quad (8)$$

$$\beta \sim (\Delta v/\Delta\sigma)/(1/c_0) \quad (9)$$

lead to an equation similar to the Arrhenius equation [eqn. (5)]. The parameters w and ϕ can be estimated for the different crystallographic directions by computing intermolecular bonds on the crystal surfaces without taking into account solvent–surface interactions.

Fig. 9 shows the crystal structure of paracetamol parallel to the (001) plane. In the paracetamol crystal lattice the O—H···O and N—H···O hydrogen bonds (thick dotted lines in the picture) link the molecules to each other to form pleated sheets {010}. The sheets are attached along the [010] axis by relatively strong van der Waals interactions (thin dotted lines). These three types of bond contribute *ca.* 60% of the entire lattice energy and define the anisotropy of the crystal lattice.

Calculations were based on the computer program HABIT[13] using 6–12 interatomic potentials.[14] The chosen set of potentials was specially derived for a variety of hydrogen bonded *N*-acetyl-*N'*-methylamides that include the same structural groups as paracetamol molecules. The following results were obtained: $(w - \phi)\ (001)_a = -16.5$ kJ mol^{-1}, $(w - \phi)\ (001)_b = -19.7$ kJ mol^{-1} and $(w - \phi)\ (110)_b = -31.3$ kJ mol^{-1}. According to eqn. (8) this means that the [100] direction on the (001) face has the greatest activation energy and the activation energy on the (110) face is the smallest.

The energy U describes the variation of critical supersaturation, σ_C, with temperature. This energy may be associated with the strength of the surface–solvent (or surface–impurity) interactions which increase along with ϕ. The calculations give the following results: $\phi(110) = 34.91$ kJ mol^{-1} and $\phi(001) = 26.86$ kJ mol^{-1}. Moreover, the (011) face has the highest density of specific water–paracetamol hydrogen bonds. This argument predicts the largest values of σ_C and U for the (110) face, as was actually observed.

Growth inclusions and mechanical properties

The changes in mechanical properties of paracetamol crystals with temperature could be due to the following.

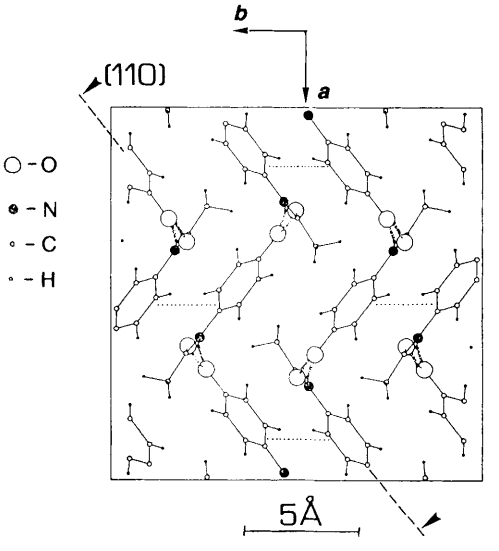

Fig. 9 Crystal structure of paracetamol crystal shown in a projection on the (001) plane. Broken lines and arrows show the most important crystal faces; dotted lines, most powerful van der Waals bond; thick dotted lines, hydrogen bonds.

(*a*) The different density of inclusions is caused by different surface kinetics of the {001} and {110} faces. The large magnitude of critical supersaturation, σ_C, for the {110} faces means that the growth steps have to overcome a barrier which may be created by a strongly adsorbed structured layer of water near the crystal surface. This results in fluctuation of growth velocity and overhanging configurations of the growth steps. A comparison between (001) and (110) crystal surfaces [Fig. 1(b) and (c)] shows that the growth steps are rough and the dislocation density is high on the (110) face. The latter corresponds to the large number of dislocation hillocks. The unstable growth conditions generally promote formation of inclusions in crystals.[11] At low temperature, the magnitude of σ_C is higher; therefore, more inclusions and poorer crystal quality can be expected at low temperature. The inclusions are probably the major factor defining the mechanical properties and are responsible for the large deviation of results during mechanical testing. The large increase of water content in the crystals (Table 1) can be directly related to the inclusion formation. Thus, for the plate-like crystals, water is mainly contained within the inclusions, whereas in the prismatic crystals it is more likely associated with the crystal lattice and is not visible under the microscope.

(*b*) Different crystal habits lead to different distributions of crystal defects. At low temperature, the imperfect {110} growth sectors become larger than the {001} sectors. As a result, the average number of defects will be higher for the low temperature crystals.

(*c*) Different crystal habits result in a crystallographic anisotropy of mechanical properties. Even the most perfect plate-like crystals exhibited lower hardness and greater plasticity than the prismatic crystals. This observation indicates that the hardness and elastic modulus are smaller for the {001} faces owing to the intrinsic crystallographic anisotropy of paracetamol. Fig. 9 shows that the direction of maximum stress (perpendicular to the crystal face under investigation) coincides with the (010) cleavage plane which favours the crushing of these crystals. In the case of the prismatic crystals, this angle is about *ca.* 38°.

Conclusions

The crystal growth and crystal quality of paracetamol have been investigated within the interval 3–50 °C and have been found to depend strongly on temperature. This temperature effect is a result of the different activation energies of the major crystallographic faces {001} and {110}. The low growth activation energy $E\{110\}$ is responsible for the transition of crystal shape from the prismatic {110} to the plate {001} as temperature decreases. The energy, U, which describes the dependence of the critical growth supersaturation on temperature, is higher for the {110} faces and explains the formation of the growth defects at a lower temperature, 3 °C. The crystallographically dependent part of the energies E and U can be estimated from the strength of the intermolecular bonds in the crystal.

The changes in mechanical properties of paracetamol crystals correlate with the growth dependences. They are related, first, to the variation of crystal habit and, second, to the formation of growth defects. The crystals with {110} dominant shape obtained at the higher temperature, 47 °C, are harder, more elastic and more resistant to fracture than the crystals with the {001} dominant shape obtained at the lower temperature, 3 °C. The defects play the major role in defining the mean value and deviation of the mechanical properties.

B.Y.S. gratefully acknowledges the financial support of this work by the Nuffield Foundation through a Research Grant to Newly Appointed Science Lecturers. The authors thank Mr R. Webster and Mr I. Lafferty for valuable technical assistance.

Glossary

$\{hkl\}$	Miller indices of a crystal form
(hkl)	Miller indices of a face
$[hkl]$	crystallographic direction
c	solution concentration
c_0	equilibrium solution concentration
D	diameter of indentor
E	activation energy of growth
E_s	activation energy of solvent complexes
E_{elast}	modulus of elasticity
Q_{elast}	elastic quotient
F	load of indentor
ΔG	Gibbs energy change
h_1	depth of the indentation
δh	elastic recovery
$\Delta_d H$	enthalpy of dissolution
HB	Brinell hardness
$\Delta_f H$	enthalpy of fusion
p	surface steepness
R	normal growth rate
R_g	gas constant
s	stress
s_C	critical stress to produce fracture
T	absolute temperature of solution
T_m	melting point
$U(hkl)$	activation energy describing dependence $\sigma_C(T)$
v	$=R/p$, tangential velocity of growth (velocity of steps)
w	energy of growth bend formation
W	work done in causing crystal fracture
β	kinetic coefficient of growth steps
ε	strain
ϕ	energy of adsorption
σ	$=\ln(c/c_0)$, supersaturation of solution
σ_C	critical σ above which crystal can grow

References

1 A. A. Chernov, L. N. Rashkovich and A. A. Mkrtchan, *Sov. Phys.-Cryst.*, 1987, **32**, 432.
2 A. A. Chernov and A. I. Malkin, *J. Cryst. Growth*, 1988, **92**, 432.
3 P. G. Vekilov, Yu. G. Kuznetsov and A. A. Chernov, *J. Cryst. Growth*, 1992, **121**, 643.
4 L. N. Rashkovich and B. Yu. Shekunov, *J. Cryst. Growth*, 1991, **112**, 183.
5 B. Yu. Shekunov, E. E. A. Shepherd, J. N. Sherwood and G. S. Simpson, *J. Phys. Chem.*, 1995, **99**, 7130.
6 D. J. W. Grant, R. I. Ristic, B. Yu. Shekunov and J. N. Sherwood, *Proceedings of the 1st International Particle Technology Forum*, AIChE, New York, 1994.
7 B. Yu. Shekunov, J. N. Sherwood and D. J. W. Grant, in preparation.
8 D. J. W. Grant, M. Mehdizadeh, A.H-L. Chow and J. E. Fairbrother, *Int. J. Pharm.* 1984, **18**, 25.
9 D. Y. T. Wong, M. E. Aulton and P. Wright, *Tabletting Technology*, 1993, **2**, 169.
10 D. Y. T. Wong, P. Wright and M. E. Aulton, *Drug Dev. Ind. Pharm*, 1988, **14**, 2109.
11 A. A. Chernov, in *Modern Crystallography III, Crystal Growth, Springer Series in Solid State Physics*, Springer, Berlin, 1984, p. 36.
12 W. C. Duncan-Hewitt and G. C. Weatherly, *J. Mater. Sci. Lett.*, 1989, **8**, 1350.
13 G. Clydesdale, R. Docherty and K. J. Roberts, *Comput. Phys. Commun.*, 1991, **64**, 311.
14 G. Nemethy, M. S. Pottle and H. A. Scheraga, *J. Phys. Chem.*, 1983, **87**, 1883.

Paper 5/04579G; *Received* 12*th July*, 1995